



Research article

Multi-omics approach for understanding the response of *Bacteroides fragilis* to carbapenems

Elena Zholdybayeva^{a,*}, Saniya Kozhakhmetova^a, Dina Bayanbek^b,
Ayzhan Bekbayeva^a, Dana Auganova^a, Gulmira Kulmambetova^a,
Pavel Tarlykov^{a,**}

^a LPP National Center for Biotechnology, Astana, 010000, Kazakhstan

^b L.N. Gumilyov Eurasian National University, Astana, 010000, Kazakhstan

ARTICLE INFO

Keywords:

Bacteroides fragilis
RNA sequencing
Meropenem
Subinhibitory concentration
Differentially expressed gene

ABSTRACT

Background: The prevalence of *Bacteroides fragilis* isolates resistant to first-line beta-lactam drugs is increasing, resulting in reduced treatment efficacy. Investigating the bacterial transcriptome and proteome can uncover links between bacterial genes and resistance mechanisms. In this study, we experimentally assessed in vitro the transcriptional and proteomic profiles of *B. fragilis* exposed to SICs of meropenem, an effective antimicrobial agent, collected from patients with intra-abdominal diseases at Astana City Hospital, Kazakhstan.

Methods: *B. fragilis* was cultured in brain heart infusion broth and sub-cultured every 48 h for 8 days in media with and without meropenem. Total RNA was extracted from the liquid cultures using a commercial RNeasy mini kit, and strand-specific RNA sequencing (RNA-seq) was performed on the DNBSEQ platform. Raw RNA-seq data were retrieved from BioProject No. PRJNA531645 and uploaded to the NCBI Sequence Read Archive (accession no. SRX22081155). Proteins of *B. fragilis* were extracted and separated using sodium dodecyl sulphate–polyacrylamide gel electrophoresis, followed by analysis of the eluted peptides using liquid chromatography–tandem mass spectrometry. Cluster analysis utilised the Database for Annotation, Visualisation, and Integrated Discovery.

Results: The subinhibitory concentration (SIC) of meropenem was determined to be 0.5 µg/L (minimum inhibitory concentration: 1). Mapping of reads to the reference genome identified 2477 expressed genes in all *B. fragilis* BFR KZ01 samples. Ten differentially expressed genes (DEGs) were common across comparison groups during and post-antibiotic exposure (wMEM vs. MEM2 and MEM2 vs. rMEM8); however, no substantially enriched Gene Ontology terms were identified. The cluster analysis highlighted a significant enrichment cluster (W-0560 oxidoreductase) of DEGs following antibiotic withdrawal. In total, 859 *B. fragilis* proteins were identified, with the expressions of three proteins, 3-oxoacyl-[acyl carrier protein] reductase, acetyl-CoA carboxylase biotin carboxylase subunit, and beta-ketoacyl-ACP synthase III, being upregulated in the enriched protein folding category. Notably, chaperone proteins such as FKBP-type peptidyl-prolyl cis-trans isomerases (involved in the cis-trans isomerisation of prolyl peptide bonds) and GroES (a co-chaperone functioning with GroEL) were also identified.

* Corresponding author.

** Corresponding author. Astana, 010000, Kazakhstan.

E-mail addresses: zholdybayeva@biocenter.kz (E. Zholdybayeva), tarlykov@biocenter.kz (P. Tarlykov).

<https://doi.org/10.1016/j.heliyon.2024.e37049>

Received 4 February 2024; Received in revised form 25 August 2024; Accepted 27 August 2024

Available online 30 August 2024

2405-8440/© 2024 Published by Elsevier Ltd.

This is an open access article under the CC BY-NC-ND license

(<http://creativecommons.org/licenses/by-nc-nd/4.0/>).

Conclusions: Under the influence of low doses of antibiotics defense mechanisms are activated which contribute to the emergence of resistance. These results provide insight into the response of *B. fragilis* to meropenem exposure, mainly at the SIC, contributing to the understanding bacterial survival strategies under stress conditions.

1. Introduction

Antimicrobial resistance remains a significant global threat to public health. In 2019, drug-resistant infections were responsible for over four million deaths worldwide [1]. Projections suggest that by 2050, antimicrobial resistance could cause up to 10 million deaths annually and incur costs exceeding \$100 trillion to the global economy [2]. Consequently, there is an urgent need for strategies to combat antimicrobial resistance.

The global prevalence of antibiotic resistance among clinical *Bacteroides fragilis* strains, which stems from the overuse of antimicrobial agents, is particularly concerning. Studies have extensively documented the worldwide increase in carbapenem and beta-lactam resistance among *B. fragilis* isolates [3]. For instance, resistance to imipenem in European countries has increased from 0 % to 1.2 % over the past two decades, with a similar trend observed in the United States [4]. Furthermore, research conducted between 2008 and 2012 indicated that 13.5 % of *B. fragilis* isolates in Taiwan exhibited resistance to ertapenem [5].

Advancements in high-throughput and innovative biological methods have significantly contributed to developments in various "omics" technologies. Multi-omics approaches have been increasingly integrated into numerous fields of biology, including microbiology. Analysing the protein profiles (proteomes) of bacterial pathogens is crucial for identifying associated proteins and understanding pathogen-host interactions, resistance mechanisms, and bacterial virulence [6]. Chernov et al. [7] have highlighted the importance of "-omics" technologies in exploring bacterial resistance mechanisms and the potential of such data to foster the development of novel antimicrobial drugs. Notably, pathogens such as *Mycobacterium tuberculosis* [8] and *Salmonella* have been the focus of multiple studies employing multi-omics approaches [9].

Carbapenems are essential antimicrobial agents used in the treatment of *B. fragilis* infections. Their mechanism of action involves penetrating the bacterial cell wall and binding to enzymes known as penicillin-binding proteins (PBPs). The primary PBP targets are 1a, 1b, 2, and 3. The binding of carbapenems to these PBPs results in the intracellular inactivation of the autolytic enzyme inhibitor, leading to detrimental effects within the bacterial cell.

Resistance to carbapenems in *B. fragilis* is primarily associated with the production of metallo- β -lactamases, which contain two Zn^{2+} ions at the active site. These enzymes are encoded by the *cfiA* gene, which can sometimes remain dormant [10–12]. There has been a noted increase in the isolation frequency of carbapenem-resistant strains of *Bacteroides* spp. The expression of *cfiA*, which mediates carbapenem resistance, is regulated by mobile genetic elements, including insertion sequence (IS) elements, such as IS1186 and IS942 with the presence of IS943 also reported [10,13].

Jamal et al. [14] conducted a study on the prevalence and susceptibility of *B. fragilis* isolates in Kuwait and found that one isolate was resistant to both imipenem and meropenem, even though *cfiA* was absent. This suggests that resistance may involve alternative mechanisms, such as alterations in bacterial membrane permeability. In recent years, bacteria have been discovered continuously develop new mechanisms of antibiotic resistance, including target defense protein, changes in cell morphology, etc., endowing them with multiple antibiotic defense systems [15,16]. Ho et al. [17] noted that resistance development to imipenem in *cfiA*-positive *B. fragilis* could be due to the expression of *cfiA* triggered by IS insertions and other not yet identified mechanisms. These potential resistance mechanisms may include mutations leading to the loss of porins, increased drug efflux, or decreased affinity for PBPs.

In their review, Yekani et al. [18] compiled data regarding the possible molecular mechanisms that underpin resistance to carbapenems in *B. fragilis*. This comprehensive review highlights the complexity of resistance mechanisms and underscores the ongoing need for detailed studies on the regulation of *cfiA* gene expression.

Recently, there has been significant interest in examining how microorganisms respond to subinhibitory concentrations (SICs) of antibiotics, which can induce varying levels of resistance. SICs are defined as antibiotic concentrations that fall below the MIC [19]. These concentrations, irrespective of the antibiotics' receptors or action mechanisms, have been observed to significantly activate transcription at low levels. SICs influence the expression levels of genes involved in primary biological processes, leading to diverse phenotypic changes in microorganisms, including changes in biosynthetic and transport processes, compound metabolism, and bacterial stress responses [20].

An analysis of the *Streptococcus pneumoniae* genome at a penicillin concentration equal to 0.5 of the mutant prevention concentration (MPC) revealed that among 386 genes with altered transcription patterns, some showed increased expression, such as those involved in cell envelope synthesis. Conversely, other genes demonstrated decreased expression, including those encoding capsular polysaccharides [21].

De Freitas and colleagues investigated the morphological, biochemical, and physiological changes, as well as the virulence of *B. fragilis* after exposure to SICs of ampicillin, ampicillin-sulbactam, clindamycin, and chloramphenicol. They discovered that the most significant morphological changes were induced by β -lactam drugs (ampicillin and ampicillin-sulbactam), which caused bacterial filamentation (elongation) of bacterial cells. Notably, the normal morphology of all strains was restored after cultivation without these antimicrobial drugs [13].

Proteomic analysis is pivotal in assessing dynamic changes in whole-protein expression at a systemic level, providing insights into the development and behaviour of resistance, as well as understanding the roles of cellular processes when pathogenic bacteria are

exposed to antibiotics. Paunkov et al. [22] conducted a proteomic analysis of metronidazole resistance in the facultative human pathogen *B. fragilis*, revealing a new hypothetical model of metronidazole resistance and the function of NimA. Furthermore, Fiebig et al. [23] utilised a multi-omics approach to identify pathways and processes that influence bile resistance in *B. fragilis*, which may promote blooming during bouts of intestinal inflammation.

Therefore, during antibiotic therapy, microbial pathogens are often exposed to low concentrations of antibiotics, creating conditions that facilitate an adaptive response. This response occurs at the transcriptional level and is expressed in ways that can enhance virulence. In this study, we experimentally assessed in vitro the transcriptional and proteomic profiles of *B. fragilis* exposed to SICs of meropenem. Our aim was to determine the relationship between bacterial genes and resistance mechanisms, as well as to identify the metabolic pathways involved in the response to meropenem.

2. Methods

2.1. Bacteria and routine culture conditions

For routine culture, bacteria were grown in Brain Heart Infusion broth (Himedia, Mumbai, India) supplemented with hemin (Sigma-Aldrich, USA, 0.5 %), vitamin K (Sigma-Aldrich, USA, 5 mg/mL), L-cysteine 0.1 % w/v (Sigma-Aldrich, USA) and meropenem (Phyto Tech Labs, USA), 0.5 µg/mL in anaerobic atmosphere at 37 °C. Cultures were let to grow until mid-log phase. As described in Fig. 1, for in vitro bacterial selection, subcultures with or without meropenem were performed in 48 h time point intervals up to 8 days. From the parent *B. fragilis* (wMEM), the MEM2 strain was selected after first subculture under meropenem pressure, and MEM8 was selected after the fourth successive subculture in the same condition. Further, rMEM2 strain was selected from MEM8 (first subculture) after drug removal, and rMEM8 strain was subsequently selected after the fourth successive subculture in the same condition. For each subculture, a 10 % in oculis was used.

2.2. Determination of subinhibitory concentration (SIC) of meropenem

Meropenem susceptibility pattern was determined by the M.I.C. Evaluator strips according to the European Committee on Antimicrobial Susceptibility Testing (EUCAST, 2023). Briefly, 0.1 mL of a 1.0 McFarland suspension of the parent strain of *B. fragilis* was spread by continuous lawn on Wilkins-Chalgren medium with increasing concentrations of meropenem ranging from 0.002 to 32 µg/mL. After 48 h of incubation, the minimum inhibitory concentration (MIC) was determined. The SIC of meropenem was considered 0.5 MIC.

2.3. RNA extraction and mRNA enrichment

Total RNA was extracted from liquid cultures of *B. fragilis* using a commercial RNeasy mini kit (Qiagen, Hilden, Germany) following the manufacturer's instructions. The RNA extracts were DNase I (Life Technologies) treated according to the RNeasy mini manual, Qiagen). To deplete prokaryotic ribosomal RNA, the MICROB Express™ Bacterial mRNA Enrichment kit (Thermo Fisher Scientific, Waltham, MA, USA) was used. RNA quality was assessed using an Agilent2100 Bioanalyzer (Agilent RNA 6000 Nano Kit; Agilent Technologies, Santa Clara, CA, USA).

2.4. RNA sequencing and transcriptomic data analysis

The RNA sequencing (RNA-seq) library was prepared using the MGIEasy RNA Library Prep Set16 RXN (MGI Tech, Shenzhen, China). Strand-specific RNA-seq was performed on the DNBSEQ platform, with a paired-end read length of 100 bp. Initially, low-quality reads were filtered out using the internal software SOAPnuke to produce "Clean Reads", which were stored in FASTQ format. The mapping of clean reads to the reference genome (*Bacteroides fragilis* NCTC_9343) was conducted using Hierarchical Indexing for Spliced Alignment of Transcripts 2 and Bowtie2 [24]. Gene expression levels were quantified using RSEM [25].

After fragments per kilobase of transcript per million mapped reads (FPKM) transformation [26], differentially expressed genes (DEGs) were identified using the EdgeR package (v3.6.8) [27]. The criteria for selecting DEGs were a fold change (FC = condition 2/condition 1 for a gene) ≥ 2 and a false discovery rate (FDR) < 0.05 . DEGs with upregulated expressions had an FDR < 0.05 and Log2 FC > 1 , whereas those with downregulated expressions had an FDR < 0.05 and Log2 FC < -1 . Volcano plots visualised the distribution of FC and FDR values for all genes between the two groups (Supplementary Fig. 1A and B,C).

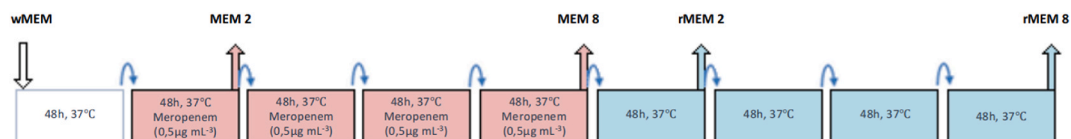


Fig. 1. Development of *Bacteroides fragilis* subcultures with and without meropenem. wMEM, parent wild-type strain; MEM2, the first stage of culture in the presence of meropenem; MEM8, the fourth stage of co-culture with the antibiotic; rMEM2, the second subculture without antibiotic; rMEM8, the fourth subculture without antibiotics.

2.5. Real-time quantification

To validate the transcriptome data, five DEGs were randomly selected for quantitative real-time PCR (qRT-PCR) assays. The RNA extraction were the same as those used for RNA-Seq. The cDNA generated from 100 ng of RNA using a **ProtoScript® II First Strand cDNA Synthesis Kit** according to the manufacturer's instructions (New England Biolabs). Reactions were conducted in 20 μ L reaction mixtures containing 1 μ L of diluted cDNA, 2 \times SsoAdvanced™ Universal SYBR® Green Supermix and gene-specific primers (**Supplementary Table S1**), nuclease free H₂O according to the manufacturer's instructions (Bio-Rad). The qPCR reactions included initial heating for 30 s at 95°C, followed by 40 cycles of 95°C, 10 s; 60°C, 30 s. The qPCR experiments were conducted on the CFX96 Touch Real-Time PCR Detection System (Bio-Rad). Three technical replicates were performed for each sample. The relative expression ratios of the target genes were calculated using the $2^{-\Delta\Delta CT}$ method using the 16S rRNA reference gene for normalization. NTC (non-template control) were used as an internal control.

2.6. Protein extraction and mass spectrometry analysis

Proteins from *B. fragilis* were extracted and separated using sodium dodecyl sulphate–polyacrylamide gel electrophoresis (SDS-PAGE). Tryptic digests were analysed using an Impact II ESI-QUAD-TOF mass spectrometer (Bruker Daltonics). Label-free quantification was performed using MaxQuant software (version 2.4.2.0). Protein quantification data were interpreted using Perseus software (version 2.0.10.0).

2.7. Protein extraction and gel electrophoresis

B. fragilis cells were harvested at three time points (wMEM, MEM2, and rMEM8) by centrifugation at 3000 \times g for 5 min at 4 °C, in triplicate. The cells were washed with lysis buffer (50 mM Tris-HCl (pH 7.4), 25 % sucrose (w/v), 1 mM PMSF, 10 mM EDTA, NP-40 (10 % v/v), 1 M MgCl₂) and harvested again under the same conditions [28]. The resulting supernatant was discarded, and the wet cell pellet was weighed. The cells were resuspended in 3 mL of lysis buffer per 1 g of cell pellet and mixed for 30 min at room temperature. Lysozyme was added at a concentration of 0.1 % (w/v), and the mixture was incubated for 35 min with gentle shaking at room temperature. In the following order, NP-40 was added to a final concentration of 0.5 % (v/v), MgCl₂ was added to a final concentration of 5 mM, and DNase I was added to a final concentration of 40 μ g/ml to the mixture. The mixture was stirred for 30 min. DNase I digests double-stranded and single-stranded DNA, reducing solution viscosity.

The samples were then centrifuged at 23,000 \times g for 30 min at 4 °C. The resulting pellet was resuspended in NuPAGE LDS sample buffer (Invitrogen, Carlsbad, CA, USA) containing 50 mM DTT. Three biological replicates were pooled in equal proportions for each time point. The soluble protein fraction (supernatant) was separated using a 4–12 % gradient NuPAGE Bis-Tris Mini Protein Gel (Invitrogen). The proteins were heated at 70 °C for 10 min before running the gel electrophoresis at 150 V for 1 h. The gels were stained with Coomassie Brilliant Blue G-250 (Bio-Rad, Hercules, CA, USA) for 1 h.

Each gel lane, corresponding to the wMEM, MEM2, and rMEM8 samples, was divided into three strips approximately 1 cm in length using disposable scalpels and transferred into microcentrifuge tubes (**Fig. 2, Supplementary Fig. 2**). The gel pieces were soaked in a

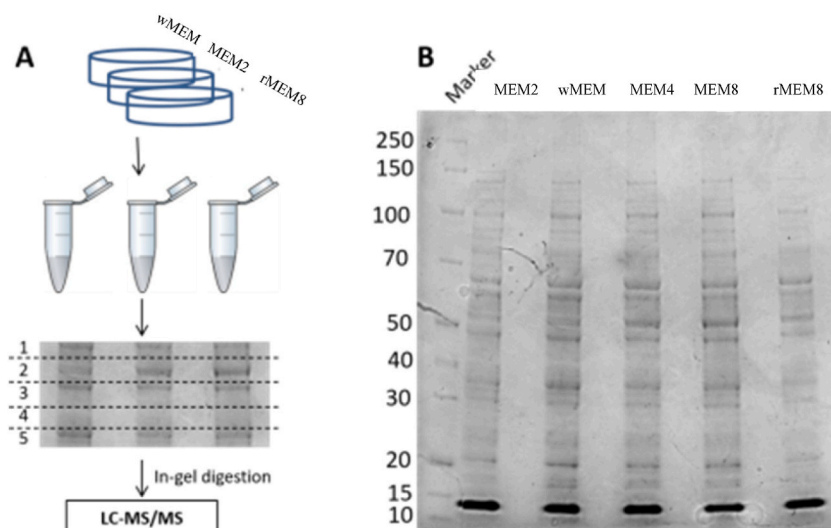


Fig. 2. *Bacteroides fragilis* protein separation using one-dimensional SDS-PAGE. WT (wMEM, wild-type; MEM2, meropenem-treated; MEM8, meropenem-treated; rMEM8, without meropenem). (a) Schematic diagram of the experimental approach. (b) SDS-PAGE analysis of *B. fragilis* extracted proteins. Proteins were separated using a 4–12 % gradient NuPAGE Bis-Tris gel and stained with Coomassie Brilliant Blue. (For interpretation of the references to colour in this figure legend, the reader is referred to the Web version of this article.)

mixture of ammonium bicarbonate (100 mM) and acetonitrile (100 %). Reduction was carried out by adding dithiothreitol (5 mM) and incubating at 60 °C for 10 min. Alkylation was performed by adding iodoacetamide (100 mM) and incubating the samples for 10 min at 37 °C. The supernatant was then discarded, and the gel pieces were washed three times with a solution containing ammonium bicarbonate (50 mM) and acetonitrile (100 %), each time incubating for 5 min at 37 °C. Following reduction and alkylation, the gel pieces were digested overnight with trypsin (20 ng/μL, Thermo Fisher Scientific, Waltham, MA, USA) at 37 °C. The peptide mixtures were purified and concentrated using a ZipTip-C18 column (Millipore, Billerica, MA, USA). Two technical replicates were analysed for each sample. The eluted peptides were dried using a centrifugal evaporator (Eppendorf, Hamburg, Germany) and resuspended in 10 μL of 0.1 % trifluoroacetic acid, then stored at –20 °C until analysis by liquid chromatography–tandem mass spectrometry (LC-MS/MS).

2.8. Mass spectrometry analysis

The mixtures were analysed using an online nanoflow-reversed-phase C18 LC-MS/MS. Chromatography was performed using a trapping column (Acclaim PepMap 100 C18 pre-column, Thermo Fisher Scientific) and a Dionex nano HPLC pump (Sunnyvale, CA, USA). The peptides were separated on an Acclaim PepMap RSLC column (Thermo Fisher Scientific) using a 75 min multistep acetonitrile gradient at a flow rate of 0.3 mL/min. An unmodified captive spray ion source (capillary 1300 V, dry gas 3.0 L/min, dry temperature 150 °C) interfaced the LC system with the Impact II ESI-QUAD-TOF mass spectrometer (Bruker Daltonics). Full-scan MS spectra were acquired at a spectral rate of 2.0 Hz, followed by MS/MS spectrum acquisition. The MS/MS peak list data were analysed using DataAnalysis 3.4 software (Bruker Daltonics) and saved in the Mascot generic format (*.mgf).

2.9. Analysis of proteomic data

The MS/MS peak lists, in Mascot generic format on a local server, were analysed using Mascot 2.6.1 software (Matrix Science, London, UK) against the Swiss-Prot protein database (release 2023_01, 569,213 sequences; 205,728,242 residues), taxonomically restricted to “Other Bacteria” containing 58,624 sequences. Search parameters included methionine oxidation as a variable modification and carbamidomethylation of cysteine residues as a fixed modification. Mass error windows of 100 ppm for MS and 0.05 Da for MS/MS were allowed.

Proteomic data were analysed using MaxQuant software (version 2.4.2.0) with the same parameters for fixed and variable modifications. Quantification was performed using a label-free algorithm. The “match between runs” feature of MaxQuant was utilised in quantification experiments for all LC-MS/MS runs, based on their masses and retention times. Data filtration, transformation, normalization, visualisation, and statistical analyses were performed using Perseus software v.2.0.10.0. Potential contaminants and proteins identified via site modifications were excluded from further analysis. Samples were filtered for 100 % valid values in each group and Student’s t-tests were performed. Missing values were replaced by values drawn from a normal distribution of 1.8 standard deviations and a width of 0.3 for each sample. Data were log₂-transformed, single peptide-identified proteins were removed, and individual values for each sample were compared using two-sample t-tests. A permutation-based FDR procedure was used to calculate q-values. Proteins with FDRs were considered significant when $q \leq 0.05$. The cut-off values for proteins with upregulated and downregulated expressions were established at two-FC (with P value ≤ 0.05) between meropenem-treated (MEM2, rMEM8) and wild-type samples.

2.10. Functional annotation

The data were functionally annotated using bioinformatic tools. Cluster analysis was performed using the Database for Annotation, Visualisation, and Integrated Discovery (DAVID; <https://david.ncifcrf.gov/>). Gene Ontology (GO) analysis is commonly used to define genes and their RNA or protein products to identify unique biological properties of high-throughput transcriptomes or genome data [29]. We visualised DEGs enriched in biological process (BP), molecular function (MF), and cellular component (CC) pathways ($P < 0.05$). UniProt Accession IDs of differentially expressed proteins were imported into DAVID for GO term enrichment analysis. Ontological analysis of GO components such as BP and MF was performed. The proteins most frequently involved in metabolic pathways were identified by associating their functional activities (EC numbers) with enzymes. Only GO terms and EC numbers that were significantly overrepresented after multiple test comparison corrections (Bonferroni correction) were considered ($P < 0.05$).

Table 1

Strains used and their sensitivity to meropenem.

Strains	Phenotype	MIC (μg/L)
wMEM	Original parent strain	1
MEM 2	Strain obtained from wMEM after first subculture with antibiotic	4
MEM 8	Strain obtained from wMEM after fourth subculture with antibiotic	4
rMEM 2	A strain derived from MEM8 as the first subculture grown under antibiotic-free conditions.	4
rMEM 8	Strain obtained from MEM8 as a fourth subculture grown under antibiotic-free conditions	4

3. Results

3.1. General characteristics of *B. fragilis* isolates

We studied a *B. fragilis* BFR KZ01 culture, isolated in 2018 from a patient diagnosed with acute gangrenous perforated appendicitis and peritonitis. The MIC of the parental strain (wMEM) was determined after 48 h of culture, with the SIC of meropenem being 0.5 µg/L (0.5 MIC).

The cells were sub-cultured with or without meropenem (Fig. 1). The strains used and their sensitivities to meropenem are listed in Table 1, with the MIC for the parent strain (wMEM) being 1 µg/L.

3.2. Sequencing data filtering and genome mapping

Full genome sequencing of this strain has previously been performed (No. SSKK01000000) [30].

RNA-Seq of the three samples was conducted using the DNB-seq platform (Table 2). Raw RNA-seq data were obtained from Bio-Project No. PRJNA531645, submitted to the NCBI Sequence Read Archive under accession no. SRX22081155. The sequence reads were mapped to the annotated *B. fragilis* NCTC 9343 sequence (NCBI: NC_003228.3; https://www.genome.jp/dbget-bin/www_bget?refseq+NC_003228). Since the initiation of the RefSeq system by NCBI in 2014, the locus-tags of most genomes, including *B. fragilis* NCTC 9343, have been updated. Therefore, "locus_tag" and "old_locus_tag" were utilised in the analysis. On average, 22.116 million reads were generated per sample. The average mapping ratios with the reference genome were 17.97 % and 12.34 %, respectively, and the quality metrics of the clean reads are documented in Table 2.

3.3. Gene mapping and expression

The mapping details are presented in Table 3. Mapping of the reads to the reference genome showed that there were 2477 expressed genes in all samples of *B. fragilis* BFR KZ01. The total numbers of transcripts identified per sample were 2326 for wMEM, 2313 for MEM2, and 2324 for rMEM8, respectively (Supplementary Table S2). For annotations, GO, and other analyses, the DAVID database used the nomenclature of the old locus tag, necessitating the use of a converter ID.

A Venn diagram illustrates the comparison of gene sets between the three groups (wMEM, MEM2, and rMEM8) and is displayed in Fig. 3. This diagram indicates that 2122 expressed genes were common to all samples, of which 2106 were annotated using the DAVID database (Supplementary Table S3).

The FPKM method was utilised to quantify gene expression levels based on RNA-seq data, accounting for the influences of sequencing depth and gene length on the number of fragments (Supplementary Table S2). To ascertain gene expression levels under different FPKM values, the expression was categorised into three ranges: FPKM ≤1, FPKM 1–10, and FPKM ≥10 (Fig. 4). Approximately 90 % of the genes exhibited an FPKM >0; approximately 6 % had a low expression level of 0 < FPKM ≤1; approximately 22 % had a moderate expression value of 1 < FPKM ≤10; and approximately 71 % showed a high expression value of FPKM >10. To further elucidate the expression profiles of the identified genes, a heat map was constructed (Supplementary Fig. 3), revealing that the expressed genes were divided into two main clusters.

3.4. Differential gene expression analysis and GO enrichment analysis

Differential gene expression analysis was conducted for three comparison groups: 1) wild-type (wMEM) vs. under the influence of the antibiotic meropenem (MEM2), 2) under the influence of the antibiotic meropenem (MEM2) vs. rMEM8 (removal of the antibiotic, cultivation for 48 h), and 3) wild-type (wMEM) vs. rMEM8. Eighty-two genes were significantly differentially expressed between wMEM and MEM2, with 47 (log₂ FC > 1, FDR <0.05) and 35 genes (log₂ FC < 1, FDR <0.05) with upregulated and downregulated expressions, respectively. A total of 78 genes showed significant differential expression between wMEM and rMEM8, with 45 (log₂ FC > 1, FDR <0.05) and 33 (log₂ FC < 1, FDR <0.05) genes with upregulated and downregulated expressions, respectively. Additionally, 95 genes were significantly differentially expressed between MEM2 and rMEM8, with 49 (log₂ FC > 1, FDR <0.05) and 46 (log₂ FC < 1, FDR <0.05) genes with upregulated and downregulated expressions (Fig. 5; Tables 4 and 5; Supplementary Tables S4, S5, S6).

The results of the GO analyses are presented in Supplementary Tables S4–S6. Data were uploaded to DAVID version 2021 for GO analysis to explore the biological functions of DEGs in the samples. Significant functional enrichment was observed, and the results are summarised in Table 6 (P < 0.05). Significantly enriched (P < 0.05) DEGs with upregulated and downregulated expressions consisted of three GO terms for molecular functions, three terms for cellular components, and two BP terms (Fig. 6). Most DEGs belonged to the functional categories of BP, including single-organism cellular processes and carboxylic acid metabolic processes. Some DEGs were

Table 2
Quality metrics of the clean reads.

Sample	Total raw reads (M)	Total clean reads (M)	Total clean bases (Gb)	Clean reads Q20 (%)	Clean reads Q30 (%)	Clean reads ratio (%)
MEM 2	24.88	23.17	2.32	97.42	90.57	93.13
rMEM 8	27.37	21.49	2.15	97.99	92.59	78.51
wMEM	24.88	21.82	2.18	97.49	90.91	87.71

Table 3
Summary of RNA-Seq mapping results.

Sample	Total clean reads	Total mapping ratio	Unique mapping ratio	Strand-specific ratio
MEM 2	23,172,534	17.56 %	12.91 %	99.68 %
rMEM 8	21,488,996	21.81 %	16.71 %	99.28 %
wMEM	21,823,604	14.54 %	10.89 %	98.79 %

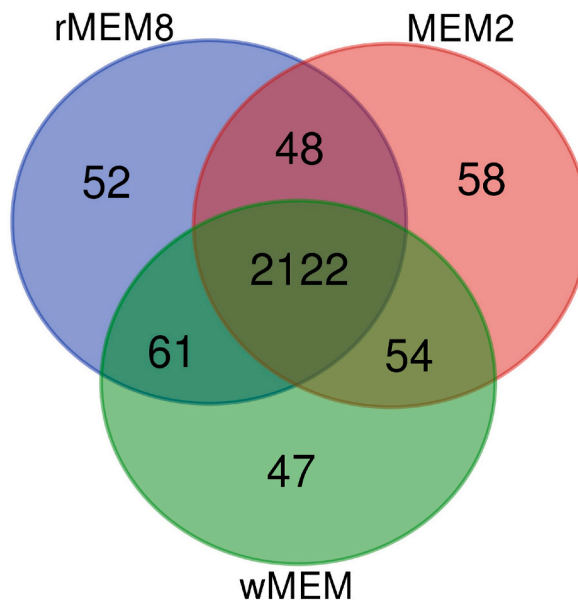


Fig. 3. Venn diagram. Overview of shared gene expression in tested *Bacteroides fragilis* subcultures (using "old_locus_tag"). Overlap of genes in three samples: wMEM - parent wild-type strain; MEM2 - the first stage of culture in the presence of meropenem; rMEM8 - the fourth subculture without antibiotics. The image was prepared using <https://bioinformatics.psb.ugent.be/webtools/Venn/>.

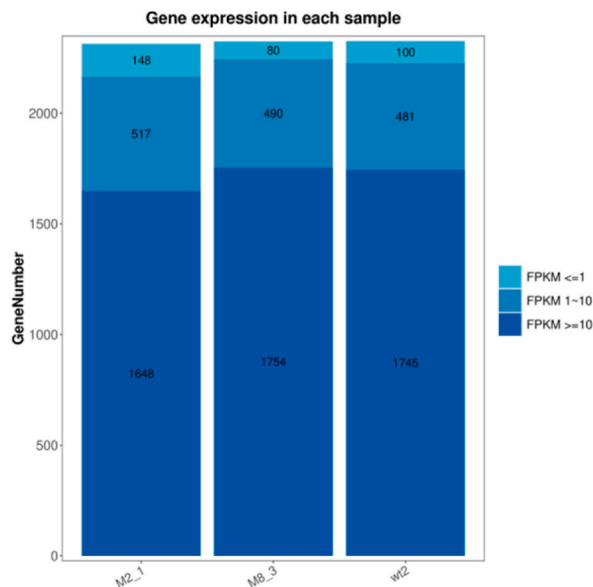


Fig. 4. Gene expression distribution. X-axis represents the sample name. Y-axis represents the gene amount. Dark colour indicates high expression level with FPKM value ≥ 10 , whereas light colour indicates low expression level with FPKM value ≤ 1 . (For interpretation of the references to colour in this figure legend, the reader is referred to the Web version of this article.)

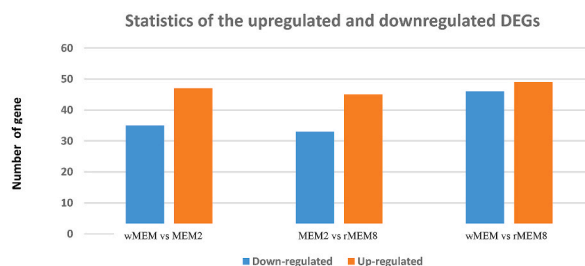


Fig. 5. Statistics of differentially expressed genes with upregulated and downregulated expressions.

related to transmembrane transporter activity, transporter activity, and hydrolase in MFs, whereas others were involved in cellular parts and the plasma membrane. The figure highlights that most genes with increased expression are related to hydrolase activity in their molecular function.

Venn diagrams were constructed for DEGs in the three comparison groups (Fig. 7). There were no common DEGs among the three groups. Notably, for the group with the parent strain under the influence of the antibiotic, only 55 genes were expressed exclusively under meropenem pressure. The number of DEGs increased to 66 after the discontinuation of antibiotics. Ten DEGs were common between the comparison groups under antibiotic exposure and after meropenem removal (wMEM vs. MEM2 and MEM2 vs. rMEM8); however, there were no significantly enriched GO terms. GO analysis revealed that 55 of the exclusively expressed genes consisted of one GO term in molecular functions, including transmembrane transporter activity and transporter activity, and the results are summarised in Table 7 ($P < 0.05$). We also analysed 66 DEGs and the results are presented in Table 8. The enrichment of up_KW_molecular_function (KW-0560 oxidoreductase) was significant. No common GO functions were detected in the comparison of genes exclusive to the strains between the groups (wMEM vs. MEM2 and MEM2 vs. rMEM8).

3.5. Validation of RNA-seq data

As shown in (Supplementary Fig. 4A and B), the qRT-PCR results revealed similar expression tendencies to the high-throughput sequencing data, despite some quantitative differences in the expression level, confirming that expression of DEGs detected using RNA-seq. A linear regression coefficient ($R^2 = 0.835$) was obtained between the FC values obtained by RNA-seq and qPCR, indicating that the RNA-seq data were reliable.

3.6. Label-free quantification of *B. fragilis* proteins

To obtain a snapshot of *B. fragilis* protein expression after meropenem treatment, we performed label-free protein quantification following SDS-PAGE separation. A total of 859 *B. fragilis* proteins were identified using LC-MS/MS. After filtering for potential contaminants and proteins identified only by site modifications, 767 proteins were retained for further analyses. Cut-off values of two-fold changes in proteins with upregulated and downregulated expressions ($P < 0.05$) were used to identify differentially expressed proteins ($n = 183$). The permutation-based FDR procedure was used to calculate q-values, and 108 proteins with FDR q-values ≤ 0.05 were considered significant. Hierarchical cluster analysis grouped the differentially expressed proteins in the meropenem-treated (MEM2 and rMEM8) and non-treated cultures of *B. fragilis* ($n = 108$) into five main clusters (Fig. 8(A and B)). Proteins identified as differentially expressed based on label-free quantification data were tabulated in Excel (Supplementary Table S7), and their gene names were used for functional annotation in DAVID.

The GO terms that were significantly overrepresented after multiple test comparison corrections (Bonferroni correction) are shown in Table 9 ($P < 0.1$). Gene functions were described using the GO terms BP and MF. Ontological analysis of the biological processes (BPs) identified significantly overrepresented proteins involved in translation (18), leucine biosynthesis (3), protein folding (3), fatty acid biosynthesis (3), and glycolysis (3) (Table 9). Ontological analysis of the MFs identified significantly overrepresented proteins involved in the structural constituents of ribosomes (18), rRNA binding (13), peptidyl-prolyl cis-trans isomerase activity (3), tRNA binding (4), and 3-isopropylmalate dehydratase activity (2).

The EC numbers that were significantly overrepresented after multiple test comparison corrections (Bonferroni correction) are presented in Table 10. EC_NUMBER 5.2.1.8 (peptidyl-prolyl isomerase) and EC_NUMBER 4.2.1.33 (3-isopropylmalate dehydratase) were the differentially expressed enzymes most frequently involved in metabolic pathways.

4. Discussion

We generated a comprehensive dataset of the genes and proteins associated with the response of *B. fragilis* BFR KZ01 to meropenem SIC. The main mechanisms of antibiotic resistance include decreased permeability of the cell membranes, which leads to disturbances in porins and protein channels in the outer membrane of gram-negative bacteria that transport various substances. Other resistance mechanisms involve the removal of antibiotics using efflux systems and enzymatic modification of antibiotic cells or the target of their action.

Table 4
The DEGs (up and down regulation) in a group wMEM vs MEM2 treated.

Molecular function	Gene ID	Protein name	log2FC (wMEM/MEM2 treated)	
Up- Regulation				
<i>transporter activity</i>	BF9343_2899	ABC transport system, exported protein (BF9343_2899)	1,59E+00	
	BF9343_2900	ABC transport system, membrane protein (bepE_1)	3,04E+00	
	BF9343_0368	Cation symporter (sglT_1)	5,02E+00	
	BF9343_1633	MFS transporter (I6J55_RS06530)	1,88E+00	
	BF9343_3418	Metal resistance related exported protein (czcB_1)	9,47E-01	
	BF9343_2505	Nramp family divalent metal transporter (I6J55_RS01110)	1,51E+00	
	BF9343_3420	Putative puter membrane protein (BF9343_3420)	1,01E+00	
	BF9343_0154	efflux RND transporter permease subunit (I6J55_RS12830)	1,06E+00	
	<i>DNA binding</i>	BF9343_3061	LacI family DNA-binding transcriptional regulator (I6J55_RS19405)	1,32E+00
		BF9343_3540	RNA polymerase sigma-70 factor (I6J55_RS16830)	8,46E-01
<i>ATP binding,</i>	BF9343_1511	response regulator transcription factor (I6J55_RS07145)	8,68E-01	
	BF9343_0485	ATP-binding component of ABC transporter (BF9343_0485)	1,72E+00	
<i>tRNA binding</i>	BF9343_2369	Putative two component system response regulator (zraR_8)	4,88E+00	
	BF9343_0109	D-aminoacyl-tRNA deacylase (dtd)	1,18E+00	
<i>thiazole synthase activity</i>	BF9343_2478	thiazole synthase (I6J55_RS01265)	2,39E+00	
<i>peptidase activity</i>	BF9343_0623	Aminopeptidase (BF9343_0623)	4,97E+00	
	BF9343_2336	Proteinase (sppA_2)	2,03E+00	
<i>sialate O-acetylerase activity</i>	BF9343_1727	Sialate O-acetylerase (estS)	9,76E-01	
<i>transferase activity</i>	BF9343_3520	4-alpha-glucanotransferase (malQ)	1,42E+00	
	BF9343_0575	Putative transmembrane acyl-transferase protein (BF9343_0575)	1,20E+00	
	BF9343_3693	sugar O-acetyltransferase (I6J55_RS16055)	1,46E+00	
<i>helicase activity</i>	BF9343_3290	ATP-dependent DNA helicase (BF9343_3290)	6,93E-01	
<i>zinc ion binding</i>	BF9343_0605	nucleoside deaminase (I6J55_RS10685)	4,99E+00	
<i>mechanically-gated ion channel activity</i>	BF9343_2995	mechanosensitive ion channel (I6J55_RS19740)	7,94E-01	
<i>antiporter activity</i>	BF9343_3501	Multidrug export protein MepA (BF9343_3501)	8,45E-01	
<i>kinase activity</i>	BF9343_0372	hypothetical protein (I6J55_RS11780)	9,63E-01	
<i>hydrolase activity</i>	BF9343_0934	metallophosphoesterase (I6J55_RS09055)	1,66E+00	
<i>xylanase activit</i>	BF9343_1273	alpha/beta hydrolase family protein (I6J55_RS07960)	2,37E+00	
<i>alpha-L-arabinofuranosidase activity</i>	BF9343_1139	Putative xylosidase/arabinosidase (xynD_3)	7,99E-01	
<i>galactosidase activity</i>	BF9343_0230	Alpha-galactosidase (aga_1)	2,71E+00	
<i>unknown function</i>	BF9343_1393	Bacteriophage-related replication protein (BF9343_1393)	5,05E+00	
	BF9343_2497	DUF169 domain-containing protein (I6J55_RS01150)	8,11E-01	
	BF9343_0291	Exported glutaminase (BF9343_0291)	1,02E+00	
	BF9343_0624	Lipoprotein (BF9343_0624)	2,88E+00	
	BF9343_3647	Liporotein (BF9343_3647)	5,07E+00	
	BF9343_3659	Membrane protein (BF9343_3659)	2,92E+00	
	BF9343_1783	Putative lipoprotein (BF9343_1783)	1,07E+00	
	BF9343_1767	Putative peptidase (BF9343_1767)	2,64E+00	
	BF9343_1640	TonB-dependent receptor (I6J55_RS06520)	3,10E+00	
	Down- Regulation			
<i>nucleic acid binding</i>	BF9343_3633	ATP-dependent DNA helicase Rec G	-1,12E+00	
	BF9343_1791	bifunctional metallophosphatase/5'-nucleotidase	-2,79E+00	
	BF9343_3571	bifunctional oligoribonuclease/PAP phosphatase NrnA	-1,26E+00	
<i>hydrolase activity</i>	BF9343_2893	ABC transport system, membrane protein (yheH)	-7,96E-01	
	BF9343_3670	MBL fold metallo-hydrolase	-9,95E-01	
	BF9343_1598	PCMD domain-containing protein	-2,35E+00	
<i>transcription factor activity</i>	BF9343_3835	GntR family transcriptional regulator	-5,11E+00	
<i>epimerase activity</i>	BF9343_0294	Aldose 1-epimerase (galM)	-1,16E+00	
<i>argininosuccinate synthase activity</i>	BF9343_0461	argininosuccinate synthase	-7,18E-01	
<i>protein tyrosine phosphatase activity</i>	BF9343_2868	Tyrosine specific protein phosphatases	-4,83E+00	
	BF9343_3575	Chloride channel protein (clcB)	-1,78E+00	
<i>voltage-gated chloride channel activity</i>				
<i>methyltransferase activity,</i>	BF9343_0858	SAM-dependent methyltransferase	-1,21E+00	
<i>dipeptidase activity</i>	BF9343_1339	Dipeptidase (pepD_3)	-1,34E+00	
<i>lyase activity</i>	BF9343_1258	Pyruvate formate-lyase-activating enzyme	-1,62E+00	
<i>isomerase activity,</i>	BF9343_1730	Lipoprotein (nanM_2)	-1,15E+00	
<i>transmembrane transporter activity,</i>	BF9343_3090	MFS transporter	-7,08E-01	
	BF9343_2338	BF9343_2338	-7,96E-01	
	BF9343_0158	DUF3108 domain-containing protein (BF9343_0158)	-9,16E-01	
	BF9343_2623	Exported TonB-dependent receptor protein (cirA_10)	-1,07E+00	
	BF9343_2323	Hydrolase	-1,15E+00	
	BF9343_2839	Membrane protein		
	BF9343_0022	PH domain-containing protein	-4,85E+00	
	BF9343_1380	Transmembrane protein	-8,79E-01	

(continued on next page)

Table 4 (continued)

Molecular function	Gene ID	Protein name	log2FC (wMEM/MEM2 treated)
	BF9343_3467	UPF0597 protein BF3560	-1,73E+00
	BF9343_3806	Uncharacterized homolog of PSP1 (-1,07E+00
	BF9343_0379	VanZ family protein	-8,83E-01
	BF9343_2455	threonine/serine exporter family protein	-1,49E+00

Although significant results were not detected, possibly due to insufficient knowledge of *Bacteroides* genes, the 10 common DEGs are of potential interest in the formation of resistance mechanisms. These 10 common genes are involved in BPs such as catabolic and carbohydrate processes, and bacteriocin immunity. A 2.14-fold upregulation of the d-aminoacyl-tRNA deacylase (dtd) gene (BF9343_0109) was observed upon both the addition and removal of the antibiotic. According to the GO analysis, BF9343_0109 is involved in chemical reactions and pathways that lead to the breakdown of d-amino acids. Geraskina et al. [31] reported that the dtd (yrvI) gene from *Bacillus amyloliquefaciens* A50, encoding the putative “metabolite proofreading” enzyme, d-tyrosyl-tRNA^{Tyr} deacylase, was associated with resistance to the non-canonical amino acid d-tyrosine. Therefore, dtd (BF9343_0109) may be involved in resistance development.

ABC transporters are assumed to play a role in nutrient uptake and drug resistance. An increase in expression of up to approximately 254.23-fold was observed in the BF9343_1139 gene, which encodes a putative xylosidase/arabinosidase (xynD_3) and participates in the carbohydrate metabolic process. Xylosidases play an important role in xylan degradation. However, its role in antibiotic resistance remains unclear [32]. There was an increase in the number of DEGs to 66 after removing the antibiotic, that is, the strain obtained from MEM8 as a fourth subculture grown under antibiotic-free conditions.

Compared to 55 DEGs under antibiotic treatment, in the study by de Freitas MCR, the authors noted that after the removal of metronidazole, the number of exclusively expressed genes increased significantly [33]. The authors concluded that even when growth conditions were restored, as in the initial state without the drug, the resulting strain underwent SIC selective pressure.

Studies have shown that in microorganisms exposed to low concentrations of antibacterial drugs, conditions are created for an adaptive response that occurs at the level of transcriptional response [20,34,35]. This leads to enhanced pathogenicity of susceptible *B. fragilis* strains subjected to low doses. In our work, strains collected after the removal of meropenem are essentially more similar to strains cultured under control conditions, supporting the fact that exposure to the drug leads to radical changes in the gene expression pattern of *B. fragilis*, and the removal of antibiotics triggers mechanisms that facilitate survival.

Destruction or modification of the antibiotic structure is one of the most effective mechanisms for resistance to enzymes. Depending on the source, the enzymes involved in this resistance mechanism are divided into hydrolases, transferases, and oxidoreductases [36]. The enrichment cluster (W-0560 oxidoreductase) of DEGs after antibiotic removal was significant. This cluster included BF9343_0082 (gluconate 5-dehydrogenase [gno]), BF9343_1318 (pirin-related protein [yhhW_2]), BF9343_0434 (putative riboflavin biosynthesis protein), and BF9343_2610 (exported methylamine utilization protein [mauG]). Therefore, oxidoreductase activity may be involved in the development of antibiotic resistance.

When comparing the results obtained from the transcriptional and proteomic analyses, it should be noted that no commonly expressed genes or proteins were identified. Although both gene expression and protein levels are genetically regulated, their correlation remains low [37–41]. Multiple studies have highlighted that even genes with similar mRNA expression levels can exhibit substantial differences in protein abundance.

Proteins that were differentially expressed in the label-free quantification data were used for functional annotation. BP and MF GO term enrichment annotated 18 ribosomal proteins with the highest group enrichment scores in the translation and structural constituents of the ribosome categories, respectively. These findings suggest that *B. fragilis* initiates a stress response upon exposure to meropenem, which disrupts cell wall synthesis. A common response is the upregulation of ribosomal proteins involved in protein synthesis and cell growth. By synthesising more ribosomal proteins, bacteria can potentially accelerate the translation of essential proteins required for cell survival. Notably, the expressions of all 18 ribosomal proteins were upregulated in meropenem-treated samples compared to those in wild-type samples. Leucine biosynthesis was also enriched among differentially expressed proteins. The upregulation of 3-isopropylmalate dehydratase may be a cellular adaptation strategy. By increasing leucine biosynthesis, *B. fragilis* might compensate for the stress caused by meropenem, thereby facilitating the maintenance of essential cellular processes and survival. A mutation in RS04935, which encodes 3-isopropylmalate dehydratase, was previously identified in *Clostridium difficile* imipenem-resistant isolates [42].

Three proteins with upregulated expressions were identified: 3-oxoacyl-[acyl carrier protein] reductase (FabG), acetyl-CoA carboxylase biotin carboxylase subunit (accC), and beta-ketoacyl-ACP synthase III (FabH). These proteins work together to ensure the proper initiation and elongation of fatty acid chains, which are essential for membrane lipid formation and various cellular processes in *B. fragilis*. Coordination between these enzymes and their respective functions is crucial for the regulation and efficiency of fatty acid biosynthesis. Meropenem disrupts these processes by inhibiting the expression of cell wall biosynthetic enzymes. Notably, multiple mutations in the *M. tuberculosis* fabG gene, which encodes 3-oxoacyl-[acyl carrier protein] reductase, have been documented as resistance mutations that impart resistance to the anti-tuberculosis drugs isoniazid and ethionamide [43]. Both drugs inhibit mycobacterial cell wall formation. When analysing DEGs, the aforementioned protein-coding genes were not identified. The bacterium responds to sudden changes in environmental conditions via radical and rapid reprogramming of the transcriptome within the first 90 min, with modest proteome changes. However, in response to gradually deteriorating conditions, the transcriptome mostly remains in

Table 5
The DEGs (up and down regulation) a group MEM2 vs rMEM8.

Molecular function	Gene ID	Protein name	log2FC (MEM2/rMEM8)
Up- Regulation			
<i>transporter activity</i>	BF9343_1852	HlyD family secretion protein (macA_3)	4,86E+00
	BF9343_1527	Outer membrane protein (bepC_1)	4,73E+00
	BF9343_0578	Outer membrane protein (tolC_3)	2,22E+00
<i>DNA binding</i>	BF9343_2901	efflux RND transporter periplasmic adaptor subunit	1,70E+00
	BF9343_2699	DNA-binding domain-containing protein	4,97E+00
<i>hydrolase activity</i>	BF9343_1881	Putative RNA polymerase ECF-type sigma factor (rpoE_15)	1,19E+00
	BF9343_3455	Acyl-ACP thioesterase	1,48E+00
	BF9343_0109	D-aminoacyl-tRNA decylase (dtd)	1,15E+00
<i>kinase activity,</i> <i>methyltransferase activity</i> <i>dehydrogenase activity</i>	BF9343_0939	arylsulfatase	3,22E+00
	BF9343_2903	signal peptidase I (lepB)	2,38E+00
	BF9343_3069	histidine kinase (yycG_1)	1,03E+00
<i>anthranilate synthase activity</i>	BF9343_3087	MGMT family protein	7,55E-01
	BF9343_2303	UDP-glucose 6-dehydrogenase (rpkK)	1,16E+00
<i>ATP binding</i> <i>beta-glucosidase activity</i>	BF9343_2590	anthranilate synthase component I family protein	2,57E+00
	BF9343_2903	signal peptidase I (lepB)	2,38E+00
<i>arabinoxylanase activity</i> <i>ATP binding</i>	BF9343_0485	ATP-binding component of ABC transporter	1,38E+00
	BF9343_0822	Beta-glucosidase (bglB)	3,07E+00
<i>arboxypeptidase activity</i> <i>electron carrier activity</i>	BF9343_0024	Exported D-alanyl-D-alanine carboxypeptidase penicillin-binding protein (dacB)	2,86E+00
	BF9343_2610	Exported methylamine utilization protein (mauG)	0,00E+00
<i>ligase activity</i> <i>lyase activity,</i> <i>arabinoxylanase activity,</i> <i>unknown function</i>	BF9343_2640	RNA ligase	4,88E+00
	BF9343_0873	O-acetylhomoserine synthase (mdeA_2)	7,84E-01
	BF9343_1139	Putative xylosidase/arabinoxylanase (xynD_3)	7,51E-01
	BF9343_0308	Conserved hypothetical exported protein	4,77E+00
	BF9343_3666	Conserved hypothetical membrane protein	3,36E+00
	BF9343_3099	Conserved hypothetical phospholipase	2,39E+00
	BF9343_2744	DUF2589 domain-containing protein	1,15E+00
	BF9343_0326	Exported protein	1,04E+00
	BF9343_3101	Exported protein	1,89E+00
	BF9343_1843	Lipoprotein	2,20E+00
	BF9343_3095	Lipoprotein	2,20E+00
	BF9343_2308	Membrane protein	7,03E-01
	BF9343_2343	Membrane protein	1,19E+00
	BF9343_3983	Predicted P-loop ATPase and inactivated derivatives	5,01E+00
	BF9343_0546	Putative TonB-linked outer membrane receptor protein	3,47E+00
	BF9343_3810	Putative transmembrane protein	1,98E+00
	BF9343_0061	Redoxin domain-containing protein	1,20E+00
	BF9343_0942	Tetratricopeptide repeat protein	4,64E+00
	BF9343_3816	TonB-dependent Receptor Plug Domain	4,78E+00
	BF9343_0093	VTT domain-containing protein	4,83E+00
	BF9343_2163	hypothetical protein	1,44E+00
	BF9343_2484	outer membrane beta-barrel protein	9,33E-01
Down- Regulation			
<i>transcription factor activity</i>	BF9343_3227	AraC family transcriptional regulator	-4,99E+00
	BF9343_0633	AraC-family regulatory protein	-1,56E+00
<i>hydrolase activity</i>	BF9343_0893	Lipoprotein (spr)	-1,12E+00
	BF9343_1598	PCMD domain-containing protein	-2,36E+00
<i>isomerase activity</i>	BF9343_1730	Lipoprotein (nanM_2)	-9,77E-01
	BF9343_1991	Peptidyl-prolyl cis-trans isomerase	-1,17E+00
<i>kinase activity</i>	BF9343_3275	hypothetical protein	-4,75E+00
	BF9343_3089	carbohydrate kinase	-8,55E-01
<i>magnesium ion bindin</i> <i>DNA polymerase activity,</i> <i>transferase activity</i>	BF9343_0761	1-deoxy-D-xylulose-5-phosphate synthase (dxs)	-7,26E-01
	BF9343_3805	DNA polymerase III subunit delta'	-7,80E-01
	BF9343_2577	amidophosphoribosyltransferase	-1,45E+00
	BF9343_3403	UDP-N-acetylglucosamine 1-carboxyvinyltransferase (murA)	-1,17E+00
<i>phosphorylase activity,</i> <i>proton antiporter activity</i>	BF9343_1084	Purine nucleoside phosphorylase/uridine phosphorylase family protein (deoD)	-7,71E-01
	BF9343_2115	Na ⁺ /H ⁺ exchanger	-1,97E+00
<i>dioxygenase activity</i> <i>zinc ion binding</i>	BF9343_1318	Pirin-related protein (yhhW_2)	-1,35E+00
	BF9343_0434	Riboflavin biosynthesis protein RibD	-4,62E+00
<i>amidase activity</i> <i>dehydrogenase activity</i>	BF9343_2698	N-acetylmuramoyl-L-alanine amidase	-4,57E+00
	BF9343_0082	Gluconate 5-dehydrogenase (gno)	-1,17E+00
<i>transporter activity</i> <i>proton antiporter activity</i>	BF9343_3070	Chromate transport protein	-1,32E+00
	BF9343_3100	cation:proton antiporter	-8,55E-01
<i>oxidoreductase activity</i> <i>dipeptidase activity</i>	BF9343_1855	cytochrome d ubiquinol oxidase subunit II(cydB)	-1,98E+00
	BF9343_1339	Dipeptidase (pepD_3)	-4,98E+00
<i>lyase activity</i>	BF9343_2473	Carboxynorspermidine/carboxyspermidine decarboxylase	-1,20E+00
	BF9343_1258	Pyruvate formate-lyase-activating enzyme (pflA)	-1,63E+00

(continued on next page)

Table 5 (continued)

Molecular function	Gene ID	Protein name	log2FC (MEM2/rMEM8)
<i>unknown function</i>	BF9343_1297	6-bladed beta-propeller	-2,16E+00
	BF9343_1524	AI-2E family transporter	-1,35E+00
	BF9343_3295	DUF5020 family protein	-4,98E+00
	BF9343_3036	Glutamyl-tRNA reductase	-1,17E+00
	BF9343_1003	LapA family protein	-4,66E+00
	BF9343_0058	Lipoprotein	-4,96E+00
	BF9343_3148	Membrane protein	-9,44E-01
	BF9343_3950	Outer membrane protein	-7,36E-01
	BF9343_0022	PH domain-containing protein	-4,95E+00
	BF9343_3164	TPR repeat domain exported protein	-8,25E-01
	BF9343_1939	Type VI secretion system needle protein Hcp	-4,72E+00
	BF9343_3467	UPF0597 protein	-1,73E+00
	BF9343_0150	hypothetical protein	-4,75E+00
	BF9343_2455	threonine/serine exporter family protein (I6J55_RS01700)	-1,52E+00

Table 6

Enrichment results of genes in clusters.

	GOTERM BP	Count	P value	Enrichment score
	<i>GO:0044763--single-organism cellular process:</i>	4	0.0375	0.767
1	BF9343_0461 (argininosuccinate synthase (argG))			
2	BF9343_0873 (O-acetylhomoserine synthase (mdeA_2))			
3	BF9343_3455 (acyl-ACP thioesterase)			
4	BF9343_3810 (putative transmembrane protein (BF9343_3810))			
	<i>GO:0019752--carboxylic acid metabolic process</i>	3	0.0544	0.767
	BF9343_0461 (argininosuccinate synthase (argG))			
	BF9343_3455 (acyl-ACP thioesterase)			
	BF9343_0873 (O-acetylhomoserine synthase(mdeA_2))			
	GOTERM CC	Count	P value	Enrichment score:
	<i>GO:0044464--cell part; GO:0005623--cell</i>	15	0.005	0.8458
1	BF9343_2473 (AraC-family regulatory protein)			
2	BF9343_3950 (carboxynorspermidine/carboxyspermidine decarboxylase)			
3	BF9343_0485 (ATP-binding component of ABC transporter)			
4	BF9343_3666 (conserved hypothetical membrane) protein			
5	BF9343_2115 (Na ⁺ /H ⁺ exchanger)			
6	BF9343_2610 (exported methylamine utilization protein (mauG))			
7	BF9343_3148 (membrane protein)			
8	BF9343_1258 (pyruvate formate-lyase-activating enzyme (pflA))			
9	BF9343_3810 (putative transmembrane protein)			
10	BF9343_0546 (putative TonB-linked outer membrane receptor protein)			
11	BF9343_0326 (putative TonB-linked outer membrane receptor protein)			
12	BF9343_2308 (membrane protein)			
13	BF9343_0109 (D-aminoacyl-tRNA deacylase (dtd))			
14	BF9343_1939, putative xylosidase/arabinosidase (xynD_3)			
15	BF9343_3070 (chromate transport protein)			
	<i>GO:0005886--plasma membrane</i>	7	0.01843	0.8458
1	BF9343_0485 (ATP-binding component of ABC transporter)			
2	BF9343_3666 (conserved hypothetical membrane) protein)			
3	BF9343_2115 ((Na ⁺ /H ⁺ exchanger)			
4	BF9343_3148 (membrane protein))			
5	BF9343_3810 (putative transmembrane protein)			
6	BF9343_3070 (chromate transport protein)			
7	BF9343_2308 (membrane protein)			
	GOTERM_MF			
	<i>GO:0022857--transmembrane transporter activity; GO:0005215--transporter activity</i>	7	0.0342	1.2820
1	BF9343_3420 (putative puter membrane protein)	7		
2	BF9343_3575 (chloride channel protein (clcB))			
3	BF9343_3501 (multidrug export protein MepA (.			
4	BF9343_0368 (cation symporter (sgIT_1))			
5	BF9343_2900 (ABC transport system, membrane protein)			
6	BF9343_2899 (ABC transport system, exported protein)			
7	BF9343_3418 (metal resistance-related exported protein (czcB_1))			

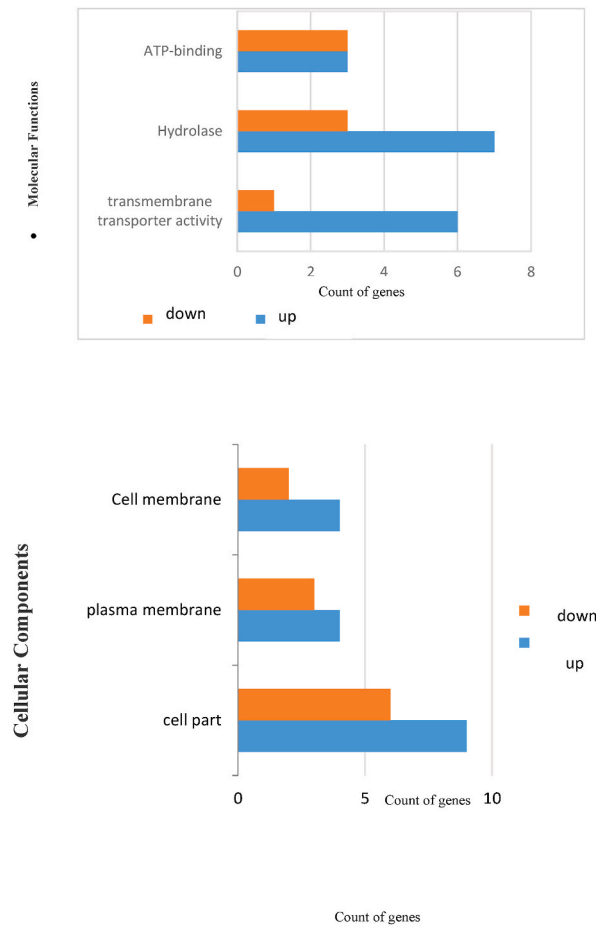


Fig. 6. Gene Ontology (GO) term enrichment analysis. Significantly enriched GO terms were selected based on an FDR <0.05. GO terms are categorised under molecular functions and cellular components.

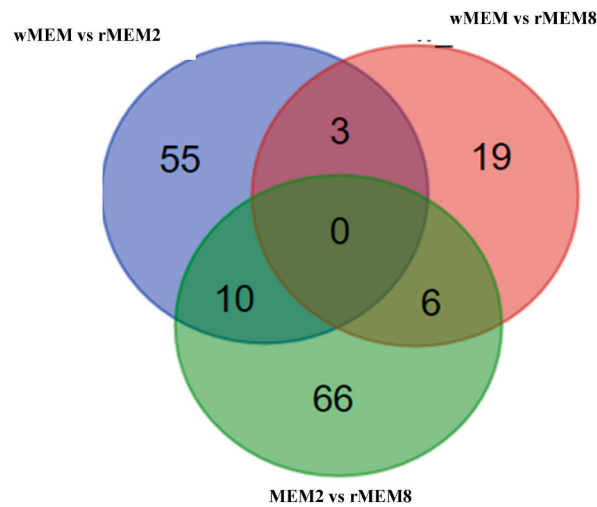


Fig. 7. Venn diagram of differentially expressed genes in the three comparison groups: wMEM vs MEM2; MEM2 vs rMEM8; wMEM vs rMEM8. Differential expression overlap.

Table 7
Enrichment results of 55 genes in clusters.

	GOTERM MF	Count	P value	Enrichment score
–	<i>GO:0022857~transmembrane transporter activity;GO:0005215~transporter activity</i>	7	0.0038	2.098
1	BF9343_3420 Putative puter membrane protein			
2	BF9343_3575 Chloride channel protein			
3	BF9343_3501 Multidrug export protein MepA			
4	BF9343_0368 Cation symporter (sgIT_1)			
5	BF9343_2900 ABC transport system, membrane protein			
6	BF9343_2899 ABC transport system, exported protein			
7	BF9343_3418 Metal resistance related exported protein (czcB_1)			

Table 8
Enrichment results of 66 genes in clusters.

	UP_KW_MOLECULAR_FUNCTION	Count	P value	Enrichment score
	<i>KW-0560~Oxidoreductase</i>	4	0.05	4.1805
1	BF9343_2610 Exported methylamine utilization protein (mauG)			
2	BF9343_0434 Riboflavin biosynthesis protein RibD			
3	BF9343_1318 Pirin-related protein (yhhW_2)			
4	BF9343_0082 Gluconate 5-dehydrogenase (gno)			
	<i>GOTERM_CC_ALL GO:0005623~cell GO:0044464~cell part</i>	11	0.034	1.669
1	BF9343_1939 Type VI secretion system needle protein Hcp			
2	BF9343_2473 Carboxynorspermidine/carboxyspermidine decarboxylase			
3	BF9343_3950 Outer membrane protein			
4	BF9343_2610 Exported methylamine utilization protein (mauG)			
5	BF9343_3666 Conserved hypothetical membrane			
6	BF9343_2115 Na ⁺ /H ⁺ exchanger			
7	BF9343_3148 Membrane protein			
8	BF9343_3070 Chromate transport protein			
9	BF9343_0326 Exported protein			
10	BF9343_0546 Putative TonB-linked outer membrane receptor protein			
11	BF9343_2308 Membrane protein			

a steady state, whereas the bacterium continues to adjust its proteome [44].

Another set of differentially expressed proteins were associated with fatty acid biosynthesis, including class II fructose-1,6-bisphosphate aldolase, cofactor-independent phosphoglycerate mutase, and type I glyceraldehyde-3-phosphate dehydrogenase. These enzymes play important roles in both glycolysis and glucose metabolism. The upregulation of the activities of these glycolytic enzymes may increase the production of glycolytic intermediates, including 3-phosphoglycerate and glyceraldehyde-3-phosphate. These metabolites can serve as precursors for various biosynthetic pathways and support the synthesis of essential cellular components, such as nucleotides, amino acids, and lipids.

Other proteins with upregulated expressions included chaperones and folding proteins, such as FKBP-type peptidyl-prolyl cis-trans isomerase, co-chaperone GroES, and trigger factors. Disruption of the cell wall by meropenem can lead to protein damage, misfolding, and unfolding, resulting in an increase in misfolded or unfolded proteins in cells [45]. In response to protein damage and misfolding, bacteria often upregulate the expressions of chaperone proteins and protein-folding factors to assist in the proper folding and refolding of damaged proteins [46,47]. These chaperone proteins include FKBP-type peptidyl-prolyl cis-trans isomerases (involved in cis-trans isomerisation of prolyl peptide bonds) and GroES (a co-chaperone that functions with GroEL). Appropriate protein folding is crucial for cellular processes including metabolism and cell survival. It should be noted that at the level of transcription of the BF9343_4195 gene, which encodes this protein, there is a statistically insignificant reduced expression.

Another key protein whose expression is upregulated in response to meropenem treatment is beta-lactam/transpept-like glutaminase. Beta-lactam antibiotics, such as meropenem, target peptidoglycan synthesis by inhibiting peptidoglycan crosslinking. This process involves enzymes known as PBPs, which are primary targets of beta-lactam antibiotics [48]. Beta-lactams or transpept-like proteins may be involved in mechanisms that mimic or compete with PBPs. In response to the disruption of peptidoglycan synthesis and inhibition of PBPs, bacteria may activate compensatory mechanisms to continue cell wall synthesis and maintain cell integrity. In addition, most DEGs identified in this study remain uncharacterized. Further studies on these transcription factor-related DEGs may improve our understanding of the molecular mechanisms underlying the defence responses.

4.1. Limitations of transcriptomics and proteomics

In our study, the limiting factor in RNA-seq was that only three samples were examined (in triplicate) due to the high costs

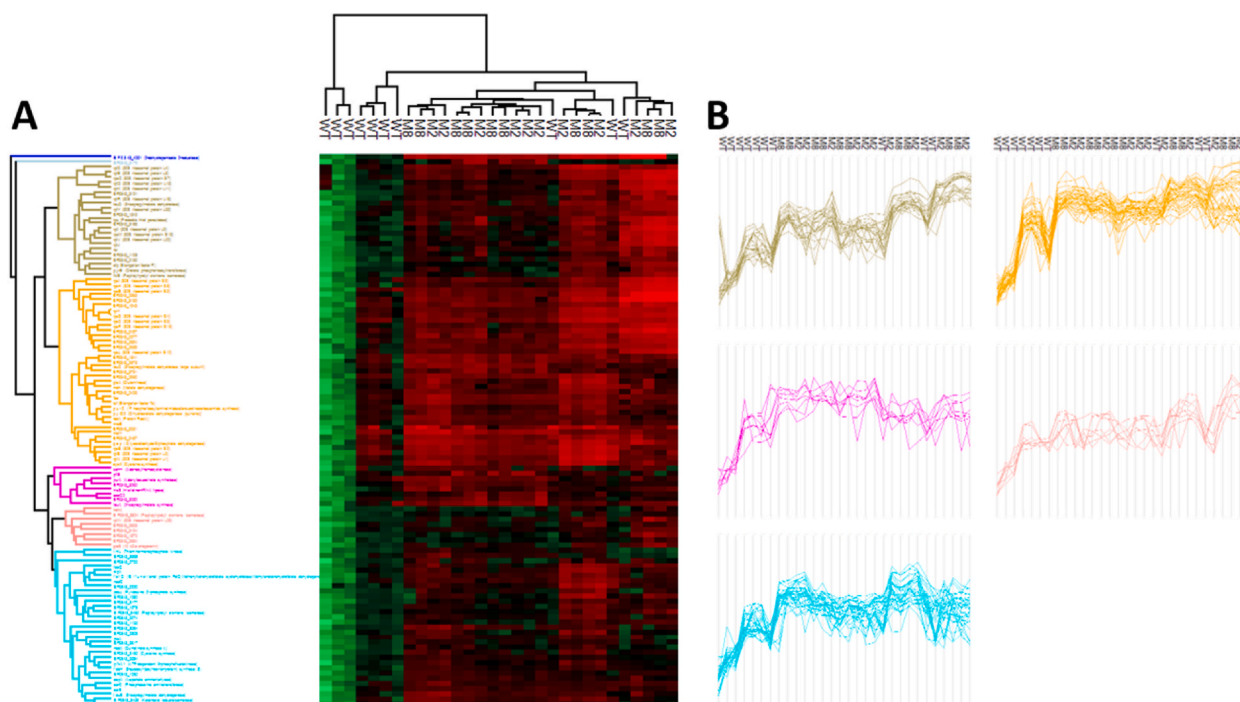


Fig. 8. Hierarchical cluster analysis (a) of 108 differentially expressed proteins in meropenem-treated (MEM2, rMEM8) and non-treated cultures of *Bacteroides fragilis*. Green indicates reduced expression; red indicates increased expression; (b) Five main clusters of differentially expressed proteins in meropenem-treated (MEM2, rMEM8) and non-treated cultures of *B. fragilis*. (For interpretation of the references to colour in this figure legend, the reader is referred to the Web version of this article.)

Table 9

Gene Ontology (GO) study of biological process and molecular function in 108 differentially expressed proteins of *Bacteroides fragilis* through functional enrichment analysis.

Category	Category name	GO term	Genes	p-value
Biological process	Translation	GO:0006412	<i>rpsM, rpsP, rpsB, rpsC, rpsD, rpsE, rpsG, rpsH, rpsI, rplA, rplK, rplO, rplR, rplB, rplV, rplY, rplD, rplE</i>	9.23E-12
	Leucine biosynthetic process	GO:0009098	<i>leuC, leuD, leuB</i>	0.023
	Protein folding	GO:0006457	<i>fabG, accC, fabH</i>	0.061
	Fatty acid biosynthetic process	GO:0006633	<i>fbaA, gpmI, gapA</i>	0.061
	Glycolytic process	GO:0006096	<i>fkpA, groES, tig</i>	0.061
Molecular function	Structural constituent of ribosome	GO:0003735	<i>rpsM, rpsP, rpsB, rpsC, rpsD, rpsE, rpsG, rpsH, rpsI, rplA, rplK, rplO, rplR, rplB, rplV, rplY, rplD, rplE</i>	5.22E-14
	rRNA binding	GO:0019843	<i>rpsM, rpsC, rpsD, rpsE, rpsG, rpsH, rplA, rplO, rplR, rplB, rplV, rplD, rplE</i>	4.68E-10
	Peptidyl-prolyl cis-trans isomerase activity	GO:0003755	<i>fkpA, fkpB, tig</i>	0.025
	tRNA bindin	GO:0000049	<i>rpsM, rpsG, rplA, rplE</i>	0.040
	3-isopropylmalate dehydratase activity	GO:0003861	<i>leuC, leuD</i>	0.064

associated with this method [49]. Most functions of the *B. fragilis* genes and proteins have not yet been determined, which complicates the GO enrichment analysis.

The quadrupole time-of-flight instrument used in this study has been the mainstay in proteomics for many years. However, many research groups have transitioned to high-resolution trapping instruments with Orbitrap analysers because of their superior resolution and mass accuracy. A total of 859 *B. fragilis* proteins were identified using LC-MS/MS. Ideally, the number of identified *B. fragilis* proteins should exceed 4,000, as the *B. fragilis* genome encodes approximately 4366 protein-coding genes. Nonetheless, achieving this number is not feasible even with high-end trapping instruments due to several proteomics limitations. Despite the limitations of mass spectrometers in terms of resolution and sensitivity, the main challenge is the dynamic range of protein abundance in the sample, which spans four to five orders of magnitude. High-abundance proteins may mask the detection of low-abundance proteins, making it difficult for mass spectrometry techniques to cover the entire dynamic range effectively. Another challenge is balancing high sensitivity (detecting low-abundance proteins) and specificity (avoiding false positives). Some proteins may escape detection due to these

Table 10

The enzymes overrepresented after the multiple test comparison correction (Bonferroni correction).

	EC_NUMBER	Count	%	P value	List total	Pop hits	Pop total	Fold enrichment	Bonferroni	FDR
	5.2.1.8 Peptidylprolyl isomerase	3	2.78	0.03	41	7	967	10.11	0.77	1.0
1	FKBP-type peptidyl-prolyl cis-trans isomerase (I6J55_RS13845)									
2	FKBP-type peptidyl-prolyl cis-trans isomerase (I6J55_RS17205)									
3	trigger factor (tig)									
	4.2.1.33	2	1.85	0.08	41	2	967	23.59	0.98	1.0
	3-isopropylmalate dehydratase									
1	3-isopropylmalate dehydratase large subunit (leuC)									
2	3-isopropylmalate dehydratase small subunit (leuD)									

trade-offs. Lastly, the incompleteness of the databases used for protein identification in proteomics is a significant hurdle. These databases are often incomplete, especially for non-model organisms such as *B. fragilis*, which include many predicted hypothetical proteins [50,51].

5. Conclusion

This work presents a comprehensive dataset of gene and protein expressions associated with the response of *B. fragilis* to SIC of meropenem. Analysis of RNA-seq data indicated that the strain selected after the removal of meropenem reverted to its original state without the drug, yet radical changes occurred in the entire structure of gene expression. There was noted an activation of the order of 7 genes, related to molecular function, *transmembrane transporter activity*, which again emphasizes the major mechanism of the resistance that includes an active exclusion of antimicrobial drugs from cells by drug transport systems. When comparing the results obtained from transcriptional and proteomic analysis, it should be noted that no common expressed genes and proteins were identified.

An increase in protein expression was observed, which, when working together contributed to ensure the proper initiation and elongation of fatty acid chains, which is essential for membrane lipid formation and various cellular processes in *B. fragilis*.

Increased expression was observed in chaperone proteins and folding proteins such as FKBP-type peptidyl-prolyl-cis-trans isomerase, GroES co-chaperone and trigger factor. Key protein is upregulated in response to meropenem treatment is beta-lactam/transpept-like glutaminase. Beta-lactams or transpeptoid-like proteins may be involved in mechanisms that mimic or compete with PBPs.

Under the influence of low doses of antibiotics defense mechanisms are activated which contribute to the emergence of resistance. These results provide insight into the response of *B. fragilis* to meropenem exposure, mainly at the SIC, contributing to the understanding bacterial survival strategies under stress conditions.

Ethics approval and consent to participate

This article does not contain any studies with human participants performed by any of the authors.

Consent for publication

Not applicable.

Funding

This research was funded by the Science Committee of the Ministry of Science and Higher Education of the Republic of Kazakhstan (grant number AP09258813).

Data availability statement

All data generated or analysed during this study are included in this published article and its additional information files. Standardized data type data have been deposited at NCBI Sequence Read Archive (SRA) data (URL <https://www.ncbi.nlm.nih.gov/sra>) with accession numbers SRX22081155.

CRedit authorship contribution statement

Elena Zholdybayeva: Writing – review & editing, Project administration, Funding acquisition, Data curation, Conceptualization. **Saniya Kozhakhmetova:** Methodology, Data curation. **Dina Bayanbek:** Methodology. **Ayzhan Bekbayeva:** Visualization, Validation, Methodology, Investigation. **Dana Auganova:** Methodology, Investigation. **Gulmira Kulmambetova:** Visualization, Software, Formal analysis. **Pavel Tarlykov:** Writing – original draft, Visualization, Methodology, Formal analysis, Data curation.

Declaration of competing interest

The authors declare that they have no known competing financial interests or personal relationships that could have appeared to influence the work reported in this paper.

Abbreviations

BP	biological process
CC	cellular component
DEG	differentially expressed gene
FC	fold change
FDR	false discovery rate
FPKM	fragments per kilobase of transcript per million mapped reads
GO	Gene Ontology
LC-MS	liquid chromatography–tandem mass spectrometry
MALDI-TOF/MS	matrix-assisted laser desorption/ionisation time-of-flight mass spectrometry
MEM2	strain selected after the first stage of culture in the presence of meropenem
MEM8	strain selected after the fourth stage of co-culture with the antibiotic
MF	molecular function
MIC	minimum inhibitory concentration
PBP	penicillin-binding protein
rMEM2	strain obtained from MEM8 (first subculture) via culture without antibiotics
rMEM8	strain derived from the fourth subculture without antibiotics
SDS-PAGE	sodium dodecyl sulphate–polyacrylamide gel electrophoresis
SIC	subinhibitory concentration
wMEM	parent wild-type strain

Appendix A. Supplementary data

Supplementary data to this article can be found online at <https://doi.org/10.1016/j.heliyon.2024.e37049>.

References

- [1] Antimicrobial Resistance Collaborators, Global burden of bacterial antimicrobial resistance in 2019: a systematic analysis, *Lancet* 399 (10325) (2022) 629–655, [https://doi.org/10.1016/S0140-6736\(21\)02724-0](https://doi.org/10.1016/S0140-6736(21)02724-0).
- [2] T.R. Walsh, A.C. Gales, R. Laxminarayan, P.C. Dodd, Antimicrobial resistance: addressing a global threat to humanity, *PLoS Med.* 20 (2023) e1004264, <https://doi.org/10.1371/journal.pmed.1004264>.
- [3] S. Jasemi, M. Emaneini, Z. Ahmadijad, M.S. Fazeli, L.A. Sechi, F. Sadeghpour Heravi, et al., Antibiotic resistance pattern of *Bacteroides fragilis* isolated from clinical and colorectal specimens, *Ann. Clin. Microbiol. Antimicrob.* 20 (2021) 27, <https://doi.org/10.1186/s12941-021-00435-w>.
- [4] G.N. Hartmeyer, J. SÓki, E. Nagy, U.S. Justesen, Multidrug-resistant *Bacteroides fragilis* group on the rise in Europe? *J. Med. Microbiol.* 61 (2012) 1784–1788, <https://doi.org/10.1099/jmm.0.049825-0>.
- [5] Q. Gao, S. Wu, T. Xu, X. Zhao, H. Huang, F. Hu, Emergence of carbapenem resistance in *Bacteroides fragilis* in China, *Int. J. Antimicrob. Agents* 53 (2019) 859–863, <https://doi.org/10.1016/j.ijantimicag.2019.02.017>.
- [6] C.R. Lee, J.H. Lee, K.S. Park, B.C. Jeong, S.H. Lee, Quantitative proteomic view associated with resistance to clinically important antibiotics in Gram-positive bacteria: a systematic review, *Front. Microbiol.* 6 (2015) 828, <https://doi.org/10.3389/fmicb.2015.00828>.
- [7] V.M. Chernov, O.A. Chernova, A.A. Mouzykantov, L.L. Lopukhov, R.I. Aminov, Omics of antimicrobials and antimicrobial resistance, *Expert Opin. Drug Discov.* 14 (2019) 455–468, <https://doi.org/10.1080/17460441.2019.1588880>.
- [8] W. Wei, H. Yan, J. Zhao, H. Li, Z. Li, H. Guo, et al., Multi-omics comparisons of p-aminosalicylic acid (PAS) resistance in folC mutated and un-mutated *Mycobacterium tuberculosis* strains, *Emerg. Microb. Infect.* 8 (2019) 248–261, <https://doi.org/10.1080/22221751.2019.1568179>.
- [9] C. Ansong, B.L. Deatherage, D. Hyde, B. Schmidt, J.E. McDermott, M.B. Jones, et al., Studying Salmonellae and Yersinia host–pathogen interactions using integrated omics and modeling, *Curr. Top. Microbiol. Immunol.* 363 (2013) 21–41, https://doi.org/10.1007/82_2012_247.
- [10] M. Kierzkowska, A. Majewska, K. Karłowicz, H. Pituch, Phenotypic and genotypic identification of carbapenem resistance in *Bacteroides fragilis* clinical strains, *Med. Microbiol. Immunol.* 212 (3) (2023) 231–240, <https://doi.org/10.1007>.
- [11] S. Jevecica, J. SÓki, M. Mueller Premru, E. Nagy, L. Papst, High prevalence of division II (cfiA positive) isolates among blood stream *Bacteroides fragilis* in Slovenia as determined by MALDI-TOF MS, *Anaerobe* 58 (2019) 30–34, <https://doi.org/10.1016/j.anaerobe.2019.01.011.s00430-023-00765-w>.
- [12] J. SÓki, E. Fodor, D.W. Hecht, R. Edwards, V.O. Rotimi, I. Kerekes, et al., Molecular characterization of imipenem-resistant, cfiA-positive *Bacteroides fragilis* isolates from the USA, Hungary and Kuwait, *J. Med. Microbiol.* 53 (2004) 413–419, <https://doi.org/10.1099/jmm.0.05452-0>.
- [13] M.C.R. de Freitas, et al., *Bacteroides fragilis* response to subinhibitory concentrations of antimicrobials includes different morphological, physiological and virulence patterns after in vitro selection//Microbial, Pathogenesis 78 (2015) 103–113, <https://doi.org/10.1016/j.micpath.2014.12.002>.
- [14] W. Jamal, F.B. Khodakhast, A. AlAzmi, J. Soki, G. AlHashem, V.O. Rotimi, Prevalence and antimicrobial susceptibility of enterotoxigenic extra-intestinal *Bacteroides fragilis* among 13-year collection of isolates in Kuwait, *BMC Microbiol.* 20 (2020) 14, <https://doi.org/10.1186/s12866-020-1703-4>.
- [15] F. Zhang, W. Cheng, The mechanism of bacterial resistance and potential Bacteriostatic strategies, *Antibiotics (Basel)* 8 (2022), <https://doi.org/10.3390/antibiotics11091215>, 11(9):1215.
- [16] G. Arora, A. Bothra, G. Prosser, K. Arora, A. Sajid, Role of post-translational modifications in the acquisition of drug resistance in *Mycobacterium tuberculosis*, *FEBS J.* 288 (11) (2021) 3375–3393, <https://doi.org/10.1111/febs.15582>.

- [17] P.L. Ho, C.Y. Yau, Y. Wang, K.H. Chow, Determination of the mutant-prevention concentration of imipenem for the two imipenem-susceptible *Bacteroides fragilis* strains, Q1F2, Int. J. Antimicrob. Agents 51 (2018) 270–271, <https://doi.org/10.1016/j.ijantimicag.2017.08.004>.
- [18] M. Yekani, M.A. Rezaee, S. Beheshtirouy, H.B. Baghi, A. Bazmani, A. Farzinazar, et al., Carbapenem resistance in *Bacteroides fragilis*: a review of molecular mechanisms, Anaerobe 76 (2022) 102606, <https://doi.org/10.1016/j.anaerobe.2022.102606>.
- [19] Ramsay KA, McTavish SM, Wardell SJT, Lamont IL. The effects of sub-inhibitory antibiotic concentrations on *Pseudomonas aeruginosa*: reduced susceptibility due to mutations. Front. Microbiol. 2021;12:789550. doi: 10.3389/fmicb.2021.789550.
- [20] L. Laureti, et al., Bacterial responses and genome instability induced by subinhibitory concentrations of, Antibiotics, Antibiotics (Basel) 2 (1) (2013) 100–114.
- [21] P.D. Rogers, et al., Gene expression profiling of the response of *Streptococcus pneumoniae* to penicillin, J. Antimicrob. Chemother. 59 (4) (2007) 616–626. <https://doi.org/10.1093/jac/dkl560>.
- [22] A. Paunkov, K. Hummel, D. Strasser, J. Söki, D. Leitsch, Proteomic analysis of metronidazole resistance in the human facultative pathogen *Bacteroides fragilis*, Front. Microbiol. 14 (2023) 1158086, <https://doi.org/10.3389/fmicb.2023.1158086>.
- [23] A. Fiebig, M.K. Schnizlein, S. Pena-Rivera, F. Trigodet, A.A. Dubey, M. Hennessy, et al., Multi-omics analysis of a *Bacteroides fragilis* isolate from an ulcerative colitis patient defines genetic determinants of fitness in bile, bioRxiv (2023), <https://doi.org/10.1101/2023.05.11.540287>.
- [24] B. Langmead, S.L. Salzberg, Fast gapped-read alignment with Bowtie 2, Nat. Methods 9 (2012) 357–359, <https://doi.org/10.1038/nmeth.1923>.
- [25] B. Li, C.N. Dewey, RSEM: accurate transcript quantification from RNA-Seq data with or without a reference genome, BMC Bioinf. 12 (2011) 323, <https://doi.org/10.1186/1471-2105-12-323>.
- [26] C. Trapnell, B.A. Williams, G. Pertea, A. Mortazavi, G. Kwan, M.J. van Baren, et al., Transcript assembly and quantification by RNA-Seq reveals unannotated transcripts and isoform switching during cell differentiation, Nat. Biotechnol. 28 (2010) 511–515, <https://doi.org/10.1038/nbt.1621>.
- [27] M.D. Robinson, D.J. McCarthy, G.K. Smyth, edgeR: a bioconductor package for differential expression analysis of digital gene expression data, Bioinformatics 26 (2010) 139–140, <https://doi.org/10.1093/bioinformatics/btp616>.
- [28] J. Richard, Simpson Large-scale extraction of recombinant proteins from bacteria, Cold Spring Harb. Protoc. 1 (2010) prot5484, <https://doi.org/10.1101/pdb.prot5484>, 2010(9):pdb.
- [29] B.T. Sherman, M. Hao, J. Qiu, X. Jiao, M.W. Baseler, H.C. Lane, et al., DAVID: a web server for functional enrichment analysis and functional annotation of gene lists (2021 update), Nucleic Acids Res. 50 (2022) W216–W221, <https://doi.org/10.1093/nar/gkac194>.
- [30] S. Kozhakhmetova, E. Zholdybayeva, P. Parlykov, S. Atavliyeva, T. Syzydykov, A. Daniyarov, K. Mukhtarova, Y. Ramankulov, Determinants of resistance in *Bacteroides fragilis* strain BFR_KZ01 isolated from a patient with peritonitis in Kazakhstan, J Glob Antimicrob Resist 25 (2021) 1–4, <https://doi.org/10.1016/j.jgar.2021.02.022>.
- [31] N.V. Geraskina, I.A. Butov, Y.A. Yomantas, N.V. Stoynova, The *tdt* gene from *Bacillus amyloliquefaciens* encodes a putative D-tyrosyl-tRNA^{Tyr} deacylase and is a selectable marker for *Bacillus subtilis*, Microbiol. Res. 171 (2015) 90–96, <https://doi.org/10.1016/j.micres.2014.11.001>.
- [32] Parmeshwar Vitthal Gavande, Shyam Ji, Vânia Cardoso, Carlos M.G.A. Fontes, Arun Goyal Reassigning the role of a mesophilic xylan hydrolysing family GH43 β -xylosidase from *Bacteroides ovatus*, BoExXyl43A as exo- β -1,4-xylosidase, Current Research in Biotechnology (2024), <https://doi.org/10.1016/j.crbiot.2024.100191>.
- [33] M.C.R. de Freitas, J.A. Resende, A.B. Ferreira-Machado, G.D. Saji, A.T. De Vasconcelos, V.L. Silva, et al., Exploratory investigation of *Bacteroides fragilis* transcriptional response during in vitro exposure to subinhibitory concentration of metronidazole, Front. Microbiol. 7 (2016) 1465, <https://doi.org/10.3389/fmicb.2016.01465>.
- [34] P. David Rogers, Teresa T. Liu, Katherine S. Barker, George M. Hilliard, B. Keith English, Justin Thornton, Edwin Swiatlo, S. Larry, McDaniel Gene expression profiling of the response of *Streptococcus pneumoniae* to penicillin, J. Antimicrob. Chemother. 59 (4) (2007) 616–626, <https://doi.org/10.1093/jac/dkl560>.
- [35] C.G. Diniz, R.M. Arantes, D.C. Cara, F.L. Lima, J.R. Nicoli, M.A.R. Carvalho, et al., Share Enhanced pathogenicity of susceptible strains of the *Bacteroides fragilis* group subjected to low doses of metronidazole, Microb. Infect. 5 (1) (2003) 19–26, [https://doi.org/10.1016/s1286-4579\(02\)00052-7](https://doi.org/10.1016/s1286-4579(02)00052-7), 2003.
- [36] A.M. Egorov, M.M. Ulyashova, M.Y. Rubtsova, Bacterial enzymes and antibiotic resistance, Acta Naturae 10 (2018) 33–48.
- [37] J. Pott, et al., Genetically regulated gene expression and proteins revealed discordant effects, PLoS One 17(5) (2022) e0268815, PMID: 35604899.
- [38] Raquel de Sousa Abreu, Luiz O. Penalva, M. Edward, Marcotte and Christine Vogel Global signatures of protein and mRNA expression levels, Biosyst 5 (2009) 1512–1526. <https://pubs.rsc.org/en/content/articlelanding/2009/mb/b908315d>. Mol.
- [39] C. Vogel, et al., Insights into the regulation of protein abundance from proteomic and transcriptomic analyses, Nat. Rev. Genet 13 (13) (2012) 227–232. PMID: 22411467.
- [40] D. Greenbaum, et al., Comparing protein abundance and mRNA expression levels on a genomic scale, Genome Biol 4 (9) (2003), 117, PMID: 12952525.
- [41] Di Zhang, Sophia Hsin-Jung Li, Christopher G. King, Ned S. Wingreen, Zemer Gitai, Zhiyuan Li Global and gene-specific translational regulation in *Escherichia coli* across different conditions, PLoS Comput. Biol. 20 (18) (2022) e1010641, <https://doi.org/10.1371/journal.pcbi.1010641>, 10.
- [42] J. Isidro, A. Santos, A. Nunes, V. Borges, C. Silva, L. Vieira, et al., Imipenem resistance in *Clostridium difficile* ribotype 017, Portugal, Emerg. Infect. Dis. 24 (2018) 741–745, <https://doi.org/10.3201/eid2404.170095>.
- [43] J. Bathke, A. Konzer, B. Remes, M. McIntosh, G. Klug, Comparative analyses of the variation of the transcriptome and proteome of *Rhodobacter sphaeroides* throughout growth, BMC Genom. 20 (2019) 358, <https://doi.org/10.1186/s12864-019-5749-3>.
- [44] World Health Organization, Catalogue of Mutations in *Mycobacterium tuberculosis* Complex and Their Association with Drug Resistance: Supplementary Document, World Health Organization, Geneva, 2021.
- [45] H. Cho, T. Uehara, T.G. Bernhardt, Beta-lactam antibiotics induce a lethal malfunctioning of the bacterial cell wall synthesis machinery, Cell 159 (6) (2014) 1300–1311, <https://doi.org/10.1016/j.cell.2014.11.017>.
- [46] S. Utaida, P.M. Dunman, D. Macapagal, E. Murphy, S.J. Projan, V.K. Singh, R.K. Jayaswal, B.J. Wilkinson, Genome-wide transcriptional profiling of the response of *Staphylococcus aureus* to cell-wall-active antibiotics reveals a cell-wall-stress stimulon, Microbiology (Read.) 149 (Pt 10) (2003) 2719–2732, <https://doi.org/10.1099/mic.0.26426-0>.
- [47] A. Muthaiyan, J.A. Silverman, R.K. Jayaswal, B.J. Wilkinson, Transcriptional profiling reveals that daptomycin induces the *Staphylococcus aureus* cell wall stress stimulon and genes responsive to membrane depolarization, Antimicrob. Agents Chemother. 52 (3) (2008) 980–990, <https://doi.org/10.1128/AAC.01121-07>.
- [48] E. Gordon, N. Mouz, E. Duée, O. Dideberg, The crystal structure of the penicillin-binding protein 2x from *Streptococcus pneumoniae* and its acyl-enzyme form: implication in drug resistance, J. Mol. Biol. 299 (2000) 477–485, <https://doi.org/10.1006/jmbi.2000.3740>.
- [49] Jungwon Choi, Jungheun Hyun, Jieun Hyun, Jae-Hee Kim, Ji Hyun Lee Cost and time-efficient construction of a 3'-end mRNA library from unpurified bulk RNA in a single tube, Exp. Mol. Med. 56 (2024) 453–460, 2024.
- [50] Olga T. Schubert, Hannes L. Röst, C. Collins, George Rosenberger Quantitative proteomics: challenges and opportunities in basic and applied research, Nat. Protoc. 12 (2017) 1289–1294. <https://www.nature.com/articles/nprot.2017.040>.
- [51] Bilal Aslam, Madiha Basit, Muhammad Atif Nisar, Mohsin Khurshid, Muhammad Hidayat Rasool proteomics: technologies and their Applications, J. Chromatogr. Sci. 55 (2) (2017) 182–196, <https://doi.org/10.1093/chromsci/bmw167>.